PREDICTING AND VERIFYING DYNAMIC OCCUPANT PROTECTION

Donald Friedman
Diego Rico
Garrett Mattos
Center for Injury Research
United States
Jacqueline Paver, Ph.D.,
Consultant
United States
Paper Number 11-0090

ABSTRACT

The objective of this paper is to describe the developments that provide the basis for predicting new car occupant protection in real-world rollovers.

An analytical technique has been developed for predicting a vehicle's dynamic occupant protection performance at any severity from a Jordan Rollover System (JRS) 50-vehicle rollover test database; static test roof strength, stiffness and elasticity data; inertial-influenced impact pitch orientation; size, roll moment and geometry dimensions; and occupant protection features. Only sampling, updating and verification of the JRS database will be necessary to reflect innovative construction and protection techniques until dynamic testing is implemented.

A noteworthy finding of this study was that reducing a vehicle's major radius (i.e., its shape at the windshield) was more effective in reducing rollover deaths and injuries than increasing roof strength-to-weight ratio (SWR) above 3.0.

INTRODUCTION

Data from over 40 vehicles has been collected by the Center for Injury Research (C*f*IR) in two-sided static tests at 10º of pitch and 25º and 40º of roll. The Insurance Institute for Highway Safety (IIHS) statically tests vehicle roof strength at 5º of pitch and 25º of roll [1]. The C*f*IR has assembled a JRS test database of vehicle and dummy measurements from more than 300 rolls of over 50 different vehicles with a variety of test protocols. The National Highway Traffic Safety Administration (NHTSA) at University of Virginia (UVa) and George Washington University (GWU) has initiated finite element research programs to identify the sensitivity of rollover crash parameters and derive a real-world injury potential test protocol [2,3]. Unfortunately, modeling has its limitations and their disparities were identified between the early published modeling and the JRS database analysis.

Injury risk results have been quantified at four levels of residual roof crush from the National Accident Sampling System (NASS) and the Crash Injury Research and Engineering Network (CIREN) databases [4,5]. General correlation of injury risk and dummy injury measure criteria in JRS tests has been confirmed. The resolution of disparities has been accomplished by considering the momentum exchange between roof intrusion and neck injury as an enhanced injury criteria that is virtually independent of small variations in occupant location. This enhanced injury criteria facilitates evaluation of occupant protection features other than roof crush (e.g., increased headroom, pretensioned belts, padding and rollover-activated window curtain airbag deployment).

Comparative consumer information about injury risk and dummy injury measure performance of vehicles can be verified to any severity protocol with readily available data. Manufacturers can use the same technique to adjust and optimize rollover injury performance during the design process to a wide range of test severity protocols and occupants.

In Australasia, Europe and America rollovers account for about 3% of the crashes, and roughly 20%, 5% and 30% respectively, of fatalities [6]. Indications are that vehicle design plays a large part in these statistics. Manufacturer's response to the competitive pressures resulting from consumer safety information is 10 to 20 years faster than the regulatory process and phase-in. This prediction technique is based on available data from comparative tests. Its predicted ratings can be verified by test sampling.

The rate of change of vehicle structural characteristics in response to front and side impact crashworthiness initiatives requires current vehicle

data, the lack or inaccuracy of which can be somewhat misleading. Nevertheless, the range of the four injury potential rating levels is spread over a range of 14 inches of residual vertical intrusion; the accuracy of verification measurements is about 10%.

A pilot program of prediction and verification by JRS testing is proposed to be accomplished in 2011. All 2012 model year vehicles statically tested by IIHS will be dynamically rated at the four injury levels and verified by sample dynamic testing.

This C*f*IR analysis is part of an ongoing effort to evaluate vehicle rollover test parameters beyond the previously-investigated sensitivity of roof strength-to-weight ratio (SWR) and impact pitch angle to residual and dynamic roof crush and injury potential.

The purpose of this paper is threefold:

(1) to predict the dynamic injury potential performance of dynamically-untested vehicles from static tests and vehicle geometry;
(2) to contribute to the effort to develop a real-world rollover test protocol; and
(3) to alert government, industry and safety advocates of the lessons learned and their application to other modes, systems and occupants.

PARAMETER REVIEW AND ANALYSIS

Development of a Real-World Test Protocol

Rollover crash statistics are summarized in Figure 1. They indicate that 94% of people in rollovers are not seriously injured and that the remaining 6% are divided; about 2% each between fatalities, severe and serious injuries in 2-roll events.

The U.S. Rollover Injury Problem

• Annual Number of Rollovers	258,000	
• Number of Occupants Involved	467,000	
• Number of Fatalities	10,000	(2.1%)
Severe to Critical injuries**	12,000	(2.6%)
• Serious Injuries**	18,000	(3.9%)
(90% of serious to fatal injuries occur within two rolls.*)		
• Not Seriously Injured	427,000	(91.4%)

*NHTSA 2003 estimates. **estimated distribution from Ciren and GWU

Figure 1. Typical rollover statistics.

More than 400 rollover crash investigations identify that 80% of catastrophic injuries (AIS = 4+) occur on the far side A study of 283 serious injury NASS rollovers exhibited damage to the hood or the top of the fenders, indicating that the roll occurred with greater than 10º of pitch [7].

In the Malibu dolly rollover tests of strong-roofed vehicles at 32 mph, the roof impact speed was 21 mph with a 4-inch drop height and an average roll rate of about 6 rad/sec with 2 rolls. Figure 2 shows data from Malibu Series 1 Test 6.

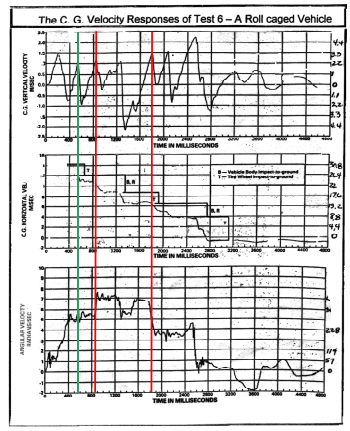

GM Malibu I
Test 6
(All data from GM Discovery)

Near Side Contacts:
(Green Lines)
575 ms = 2.2 mph
1500 ms = 2.5 mph

Far Side Contacts:
(Red Lines)
836 ms = 2.7 mph
1802 ms = 3.1 mph

Figure 2. GM Malibu I test no. 6.

Two test fixtures were developed and used to evaluate vehicle rollover performance:

- A two-sided 10º of pitch platen test, and
- A repeatable dynamic rollover machine.

The M216 two-sided fixture applies forces to the roof on one side and then the other at force angles of 10º pitch and 25º and 40º roll, respectively. The M216 results indicate that most vehicles are about half as strong compared to the FMVSS 216 test results at 5º of pitch, as shown in Figures 3 and 4.

Figure 3. M216 two-sided static test machine.

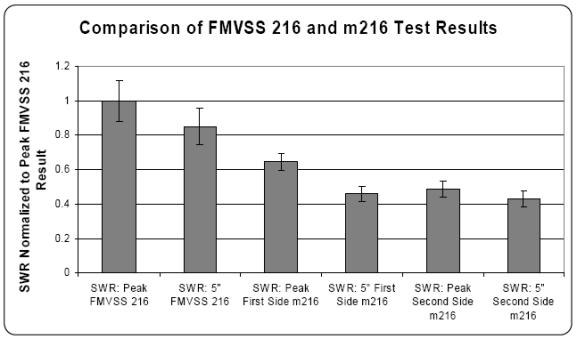

Figure 4. Two-sided NHSB/M216 data.

The JRS rollover fixture, shown in Figure 5, is a laboratory device capable of rolling full-size vehicles to 6,000 lbs at 300º/ sec, dropping them 4 to 9 inches onto a 20 mph moving roadbed and measuring the roadbed forces and roof intrusion [8].

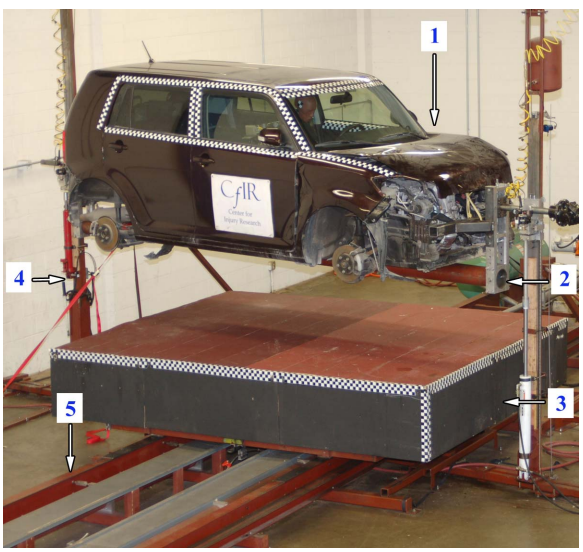

Figure 5. The JRS fixture key components: 1) vehicle, 2) cradle/spit mount, 3) moving roadbed, 4) support towers, 5) coupled pneumatic roadbed propulsion and roll drive.

With this data, these tools and tests on more than 50 vehicles, our analysis of the segments of a rollover from the loss of control, yaw to trip, trip and ballistic trajectory identified the segment 5 of Figure 6 as the most probable source of severe injury.

Segments of the Roll Sequence	Potential for Serious-to-Fatal Injury
1. Vehicle loss of control	Non-injurious
2. Yaw-to-trip orientation	Occupants move laterally out-of-position
3. Trip	Exacerbates lateral out-of-position
4. Roll rate	Potential for far-side injury and ejection
5. Vehicle roof impacts with the road	Potential for severe head/neck/spine injury
6. Wheel/underbody contacts	Potential for lower spine injuries
7. Suspension rebound and second roll lofting	Non–injurious
8. Near-side roof impact, roll slowing ejection	Potentially injurious
9. Far-side impact	Potentially injurious
10. Wheel contact to rest	Non-injurious

Figure 6. 10 segments of the roll sequence.

The result was the proposed "Real World Protocol" in Figure 7.

The Proposed Real-World Rollover Protocol

- Road speed 33 kph ± 7 kph (20 mph ±5 mph),
- Roll rate @ near-side impact 270 °/sec ± 20%
- Pitch 10° ± 5°
- Roll angle at impact 135° ± 10° and/or 185°
- Drop height 10 cm to 22 cm (4 to 9 inches)
- Yaw angle 15° ± 15°
- Dummy tethered @ 1 g and 60° toward the near side.

Figure 7. Updated proposed test protocol.

Development of Injury Measures and Criteria

Two studies 25 years apart indicate that spinal distortions and fractures, primarily in the lower neck are typical rollover injury patterns. The 1983 Allen study of severe human neck injuries attributed 60% to flexion, 30% to extension and 10% to axial compression [9]. The 2009 Ridella study of CIREN cases indicates that a predominance of serious injuries involved the spine as shown in Figure 8 [10].

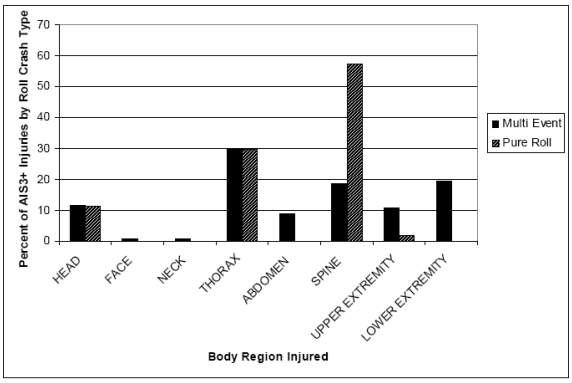

Figure 8. CIREN distribution of rollover injuries.

The measures that proved to be the most significant indicators of injury during a rollover event were the lower neck bending moments, measured at the C7-T1 level and the duration of neck bending. You can imagine a boxer receiving a blow to the face, although this could result in a large lower neck bending moment the boxer's head would move away and the peak moment would reduce rapidly. No lower neck injury would occur because the load was not sustained and did not cause the neck to bend. Lower neck bending injuries require that a large enough moment be sustained for the duration that flexs the neck beyond its physiologic range of motion [11].

Figure 9 shows the mechanism of a common neck bending Injury, a bilateral facet dislocation. It is initiated by significant flexion of the neck which dislocates the spine. It concludes with the neck contracting, pulling the spine forward and down locking the facets [11].

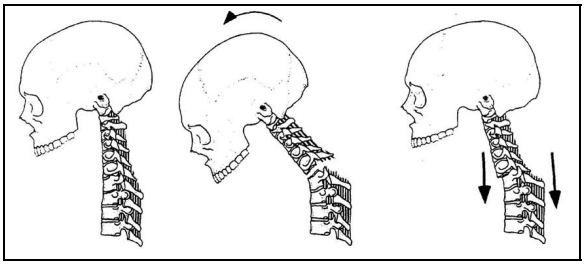

Figure 9. Hyperflexion neck injury mechanism from Pintar, et al.

This and other neck bending injuries can be predicted by looking at the area under the lower neck bending moment curve. This area is akin to the Head Injury Criteria used to determine the injury potential from a head impact. It takes into account not only the peak load but also the duration of that load.

Roof crush and the loss of headroom are directly related to the bending moment measured in the neck. In a study of over 10,000 rollover accidents it was found that the probability of spine injury increased with increased residual roof crush [12]. Table 1 is the criteria for seriously injurious peak forces in flexion and bending [13].

Table 1.
Peak lower neck IARV's for a 10% probability of an AIS≥3 injury

Neck Type	Neck Loading Direction	Axial Fz (N)	Moment My (Nm)	Moment Mx (Nm)
Production Hybrid III	Flexion	6,000	380	
Production Hybrid III	Lateral Bending	6,000		268
"Soft" Neck	Flexion	~2,000	~90	
"Soft" Neck	Lateral Bending	~1,640		~59
Human/Cadaver	Flexion	~1,500	~58	

<u>JRS injury criteria and measurements</u> In JRS tests roof movement was measured at four locations in the vehicle. The peak dynamic roof crush and residual roof crush were determined for each roll. A sampling of the JRS rollover database is provided in Appendix 1.

Figure 10 shows the 2009 Mandell studied the NASS/CIREN database and established a four level probability of injury risk as a function of vertical residual crush to 14 inches.

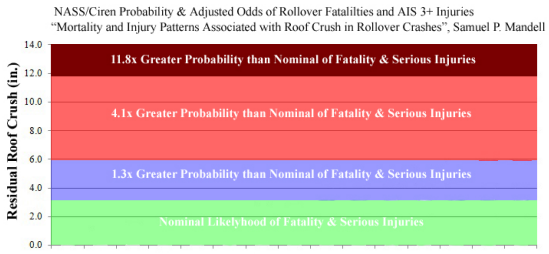

Figure 10. NASS/CIREN probability and adjusted odds.

Results of pendulum tests indicate that peak axial neck force is not a good indicator of injury to the spine. This is due to the very stiff axial and vertically-oriented neck of the Hybrid III dummy.

Flexion injury occurs from a moment applied by a 4 to 9-inch impact stroke to the top/back of the head over 40 to 140 ms [14]. Dummy peak forces and moments grossly underestimate and misrepresent the extent and duration of the required flexion injury intrusion in a rollover. That is also why the vertical residual crush correlates so well with the Integrated Bending Moment (IBM) [15].

The IBM criteria is [15] related to the amplitude and duration of the forces and moments. It integrates the resultant moment (lower My and lower Mx) over the time interval where it is greater than 30 Nm to a maximum of 140 ms for the original Hybrid III neck and proportionately less for the soft neck.

It is clear from the JRS test videos of the dummy head/neck motion that the roof of the production vehicles interact with the head of the soft neck dummy in a much more severe manner. The reinforced roofs provided much more protection by maintaining the occupant survival space. This is illustrated by superimposing the lower neck bending moment of an identical pair of production and reinforced Ford Explorers. The IBM is the respective areas under the bending time histories curves in Figure 11.

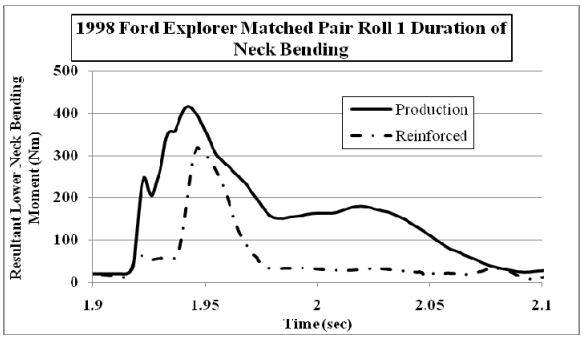

Figure 11. 1998 Ford Explorer matched pair testing roll 1.

In the JRS tests, the production vehicles sustained twice as much residual roof crush than the reinforced vehicles. This equates to an average of 5 inches more roof crush during the event.

The "soft" low musculature modified Hybrid III dummy neck shown in Figure 12 was literally broken at the lower neck load cell mount as a result of 11 inches of roof crush in this SWR 6.8 vehicle.

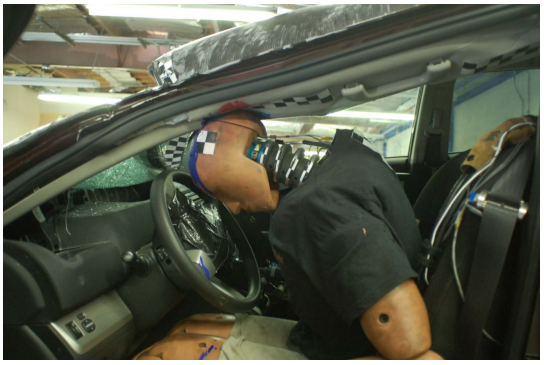

Figure 12. Soft neck of hybrid III dummy.

<u>Controlled Rollover Impact System (CRIS) tests</u> Published 15 ms video clips and neck injury measure data of production and reinforced 1998 Crown Victorias tested on the CRIS show identical results in roll-caged and production vehicles [16]. In the video dummy movement up to the point of initial roof contact is nearly identical. However**,** the videos and data to 140 ms tell a very different story. Figure 13 show the interior views. The production vehicle with the grossly bent neck is shown on the left. The deformation of the roof in the production vehicle applied a force to the head of the dummy and caused the neck to bend significantly. No neck bending was observed in the reinforced vehicle (right). Estimated roof crush is 2 inches for reinforced and more than 10 inches for the production vehicle.

Figure 13. Production vehicle's neck severely bent after 40 ms (left) and the roll-caged vehicle's non-injurious neck bending (right).

The peak lower neck bending moments measured in the production vehicles was 30 to 56% greater than in the reinforced vehicle. The duration of neck bending in the production vehicle was 150% greater for the reinforced vehicles. Dummies in the production vehicles were trapped 2 out of the 5 times in injurious positions that could limit breathing and inhibit safe evacuation [16].

<u>Critical parameters for structural intrusion</u> The mining of the JRS database for correlations of vehicle structural parameters with residual roof crush has so far identified a few of high importance and weighting in predicting injury risk. These are in order of priority SWR, major radius, pitch, elasticity and near- and far-side road load effects.

<u>Critical parameters for dummy injury measures</u> Residual and dynamic crush and crush speed are probably the most important parameters affecting neck bending and head injuries respectively. [ref} While the drop height can be important, all data indicates that automobiles and SUVs in rolling over stay close to the ground and with belted occupants have little effect compared to intrusion. The headroom in vehicles varies by about 4 inches (from 3 to 7 inches). Therefore in terms of strong-roofed vehicles with crush in the order of 6 inches or less

headroom can be significant. That same effect applies to lap and shoulder belt performance whose range is 3 to 5 inches. Pre-tensioned belts can reduce the excursion by 2 inches. Rollover-activated window curtain airbags can be important in the likely case of out-of-position far-side occupants, who may be out of their shoulder belt from yaw-to-trip forces and rebound rapidly to strike the roof rail and window as the roof crushes [17].

Normalization procedures It appears clear that the choice of a particular compliance and/or NCAP test protocol is unlikely to be a technical decision. So, it is important to be able to translate results from one protocol to characterize another. It is also important to characterize and estimate the performance of similar vehicles in a real-world crash. To that end, normalization procedures have been developed to adjust or predict the injury risk potential and injury measures for alternate road speeds with proportional roll rates, different pitches and independent road speeds and roll rates.

Structural Analysis of the JRS Database

The JRS database now has about 50 vehicles and about 300 rolls. The data was collected over the 6 operational years of the machine, where procedures, instrumentation, dummy characteristics, injury measures and criteria were changed as we learned and vehicle structures improved. In the following charts, roll 1 is at 5° pitch, roll 2 is at 10° pitch, and analyses are based only on vehicles with the same protocol whose measurements could identify correlations and their slope as it affected residual crush. In many cases this limited the number of vehicles to as few as 10. This is thought to be sufficient for a reliable insight into the factors which affect rollover injury potential, but the reader is cautioned to consider the outcomes preliminary until other scientists duplicate the results.

SWR vs. cumulative residual roof crush Figure 14 shows the generic injury measures with about the same slope as a function of SWR to 4 and injury risk to about 4 or 5%. The chart incorrectly projected the JRS test data to an SWR of 5, but subsequent tests of vehicles with SWR above 4 and to 6.8 correlate with a polynomial relationship primarily because one vehicle with an SWR of 6.8 had 10 inches of crush. In a companion paper 2011-0405 this set of data is used to demonstrate the range of these parameters that can be used to reasonably predict vehicle performance.

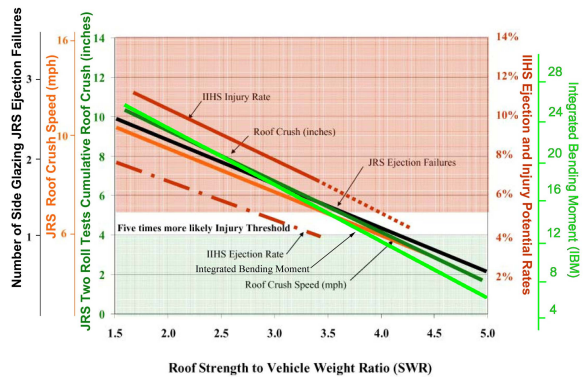

Figure 14. Roll 2: cumulative residual crash and major radius.

Other characteristics, particularly vehicle geometry and elasticity, have been identified to account for this non-linearity [18]. The current cumulative residual crush chart versus SWR is shown in Figure 15. This is still consistent with IIHS' original statistical slopes of SUVs and small passenger cars to an SWR of 4 [19].

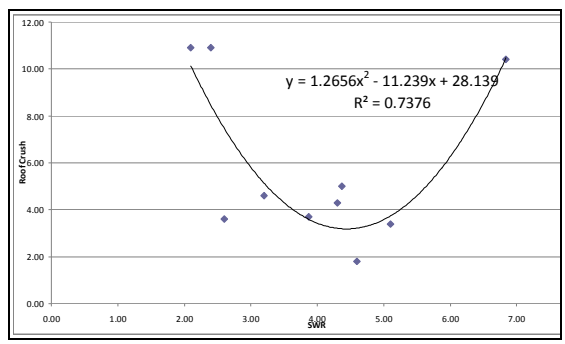

Figure 15. SWR vs. current cumulative residual roof crush.

Major radius and cumulative residual crush

The major radius of a vehicle is the distance between the CG axis and the roof rail at the A-pillar. Figure 16 identifies the vehicles involved, their major radii and the cumulative residual crush at the A-pillar in roll 1 and roll 2.

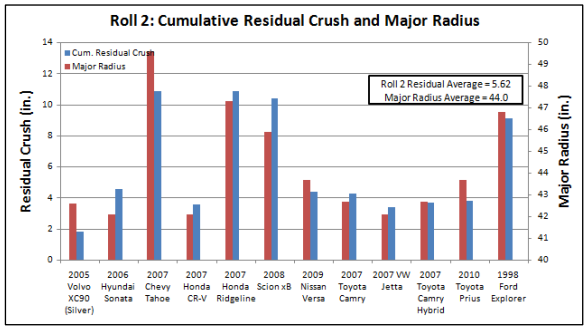

Figure 16. Major radius and cumulative residual crush.

Figure 17 is a scatter plot of the Major radii for those vehicles and indicates a high correlation with the cumulative residual crush of roll 1 and 2. The relationship is particularly striking for the slope which indicates that each 1.2 inches of major radius affects the residual crush by 1 inch. This is an enormous effect easily doubling the magnitude of residual roof crush between SUVs and automobiles. Considering IIHS studies to reduce risk by 24% for each increment of SWR, reducing the major radius of SUVs from a typical 46 inches to that of automobiles, the XC-90 and CR-V of 42 inches reduces intrusion by 3.3 inches [19].

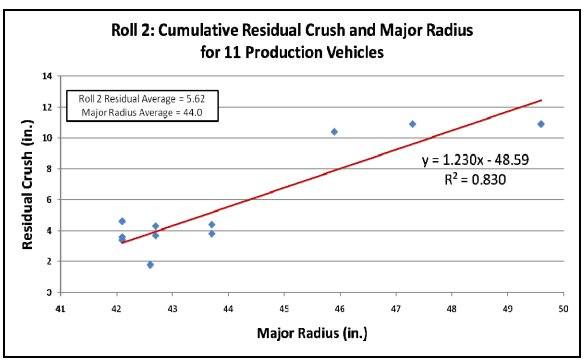

Figure 17. A scatter plot of the cumulative residual crush of roll 1 and roll 2 vs. major radius.

<u>Elasticity and cumulative residual crush</u>

Another significant effect appears to be the result of high strength steels used in the most updated vehicles. This effect became noticeable in 2007 when improved compliance with FMVSS 214 also increased the vehicle's roof SWR.

To interpret the data, vehicles with an elastic structure like the 70% Volvo XC-90 have a lesser effect on residual crush than vehicles like the 30% Scion xB which buckled and collapsed. Figure 18 shows that an elastic structure has a significant correlation and slope with residual crush. The weighting compared to SWR and major radius is as yet unknown.

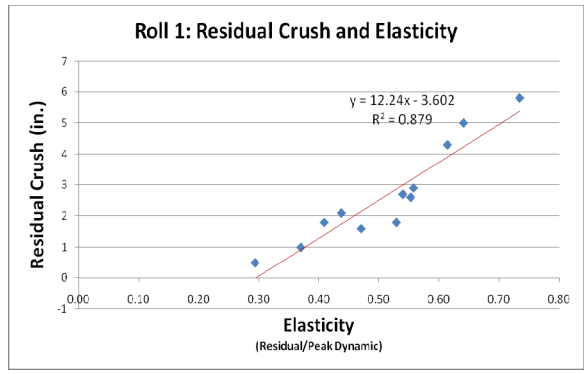

Figure 18. Roll 1 residual crush and elasticity.

Injury Measure Analysis of the JRS Database

<u>Integrated Bending Moment (IBM) and residual crush</u>

From an injury measure point of view the IBM correlates well with residual crush, with injury risk at 3.5 inches, with the 10% probability of AIS = 3+ IARV injury measure and seems insensitive to small variations of dummy head position. Three and a half (3.5) inches of residual crush corresponds to an IBM of 13.5 as shown in Figure 19.

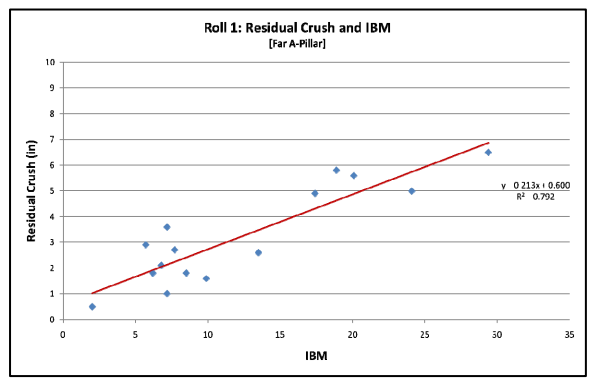

Figure 19. Roll 1: Residual crush and IBM [far A-pillar].

<u>Headroom vs. residual crush</u>

When considering dummy injury measures headroom is significant as shown in Figure 20.

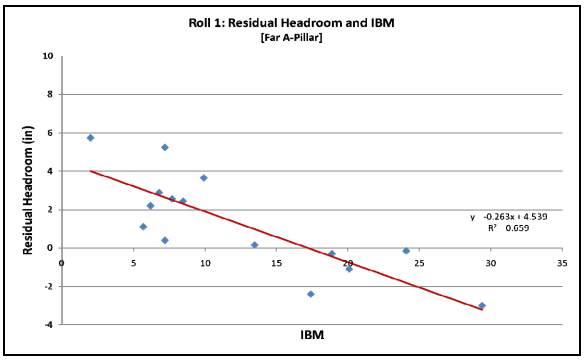

Figure 20. Headroom vs. residual crush

<u>Belt loads, excursion and pretensioning</u> Belt loads and corresponding excursions have been measured on many tests but not yet correlated with IBM for this paper. Excursion varied from 3 to 5 inches with occupant size and weight. Pretensioning reduces excursion by about 2 inches.

<u>Road speed and proportional roll rate</u> There is a high correlation between average residual crush and road speed with proportional roll rate as shown in Figure 21. The roll rate proportionality comes from the JRS I configuration where the road speed and roll rate are geared together. One test was performed with an alternate ratio resulting in a 15 mph and 303 deg/sec roll rate.

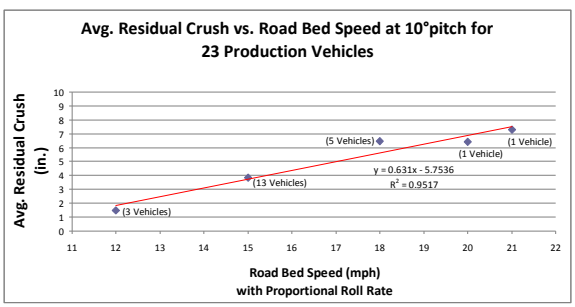

Figure 21. Average residual crush vs. road bed speed.

<u>Road speed vs. roll rate</u> There is insufficient data to resolve the contribution of road speed and roll rate separately. The data that is available is shown in Table 2. A few identical separate vehicles have been tested under slightly different circumstances. The first of a pair of GMC Jimmys, at 5º of pitch, when tested at 10º of pitch shows a 32% increase in dynamic intrusion.

Table 2.
Road speed vs. roll rate

			Protocol			Far A		
	Test #	SWR	Pitch	Road Speed	Roll Rate at impact (deg/s)	Peak Dynamic (in)	Residual (in)	Speed (mph)
1996 GMC Jimmy	1	1.6	5	15	188	6.3	4.2	5.2
2000 GMC Jimmy	1	1.6	10	15	174	8.3	7.2	6
				Percent Increase		32	71	15

			Protocol			Far A		
	Test #	SWR	Pitch	Road Speed	Roll Rate at impact (deg/s)	Peak Dynamic (in)	Residual (in)	Speed (mph)
1999 Hyundai Sonata	1	2.8	5	15	172	6.4	4.5	5.5
1999 Hyundai Sonata	1	2.8	10	21	275	10.9	7.3	13.2
				Percent Increase		70	62	140

			Protocol			Far A		
	Test #	SWR	Pitch	Road Speed	Roll Rate at impact (deg/s)	Peak Dynamic (in)	Residual (in)	Speed (mph)
1998 Ford Explorer	1	1.9	5	15	183	7	4.3	4.4
2000 Ford Explorer	1	1.9	5	15	200	8.7	5.9	6.3
1998 Ford Explorer [Reinforced]	1		5	15	177	1.9	0.8	4.2

The first of a pair of Hyundai Sonatas shows a 70% increase in dynamic intrusion for both an increase to 10 deg pitch and a 21 mph road speed with proportional roll rate.

Lastly are listed three Ford Explorers (with and without sun roofs accounting for the difference in intrusion), one vehicle was reinforced and had 25% of the roof intrusion of the production vehicles. This confirmed that increased roof strength reduces intrusion.

The point is that if 10º pitch accounts for 30% (the Jimmy's) and pitch and speed with proportional roll rate (the Hyundai's) accounts for 70%, then the speed and proportional roll rate accounts for 40% for a speed and proportional roll rate increase of 40% (from 15 to 21 mph) as shown in Figure 21.

Still unresolved is whether that 40% increase is from increased road speed or roll rate. There is only one test at 15 mph, 5 deg pitch, 125 deg impact angle and 303º roll rate, a 1999 Camry, which could resolve that issue. The other tests were at 145 deg and 190 deg /sec. Previous 125 deg impact angle tests resulted in nearly equal near and far side road loads and intrusion. For the 1999 Camry the road loads and intrusion were very much greater on the far side. The 1999 Sonata and Camry are both estimated to have SWRs of about 2.8, yet the Camry residual crush of 7 inches shown in Figure 22 suggests that low impact angle and high roll rate result in a similar 7.3 inches of intrusion as the 21 mph and 280 deg/sec test. Finite element tests of a strengthened (SWR = 3.9) Explorer in a private communication indicated about the same dynamic intrusion in combinations of 40% increased speed and roll rate.

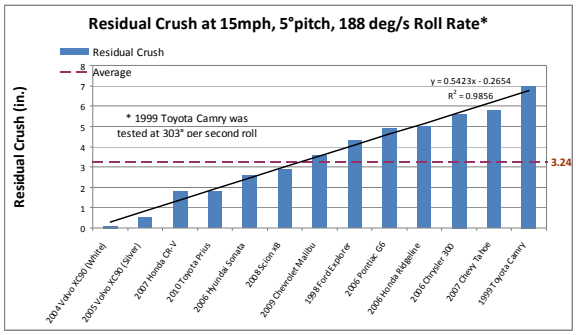

Figure 22. Residual crush at 15mph, 5º pitch, 188 deg/s roll rate.

<u>Pitch and CG location</u> Pitch has been shown by JRS tests to be a highly sensitive parameter to roof crush. The difference in roof crush between 5 deg of pitch and 10 deg of pitch in JRS tests has typically been shown to be quite substantial. Most JRS tests are done in a 2 roll sequence in which the first roll is performed at 5 deg of pitch and the second roll is performed at 10 deg of pitch. The question is what vehicle parameter or characteristics would make a vehicle roll with a large degree of pitch. One explanation is that generally fully-loaded vehicles roll with little or no pitch. Taking this into consideration it would make sense that the location of the center of gravity (CG) of a vehicle relative to its A-pillars and pivot point is an important characteristic in determining the likelihood that a vehicle would roll with a pitch of 10º or greater. In theory, a vehicle whose CG is farther back from its A-pillars and behind its pivot point will likely roll flat on its roof. Thus the normal force of the road would be spread out over a larger surface area and result in less roof crush. A vehicle whose CG is closer to the A-pillars and forward of the pivot point will have a greater likelihood of rolling with a substantial pitch and thus result in greater roof crush. Both of these situations are illustrated below in Figure 23.

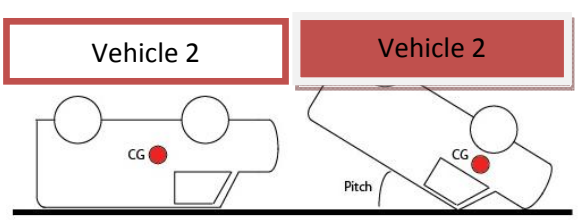

Figure 23. Illustration of the two rollover situations.

The distance between the CG and the A-pillar were calculated for several unloaded vehicles and tabulated in columns 1 to 4 in Table 3. (Note that a negative horizontal distance value implies that the CG is behind the A-pillar and vice versa for a positive value.)

Table 3.
CG distances relative to A-pillar

Vehicle	Horizontal Distance between CG and Top of A-pillar (in.)	Vertical Distance between CG and Top of A-pillar (in.)	Normal (90°) Distance between CG and Top of A-pillar (in.)	Horizontal Distance between CG and Virtual A-pillar (in.)
2008 Scion xB	-12.7	38.2	40.3	-5.7
2009 Chevrolet Malibu	-2.7	34.6	34.7	3.3
2009 Nissan Versa	-5.8	36.8	37.3	0.7
2007 Honda CR-V	-6.3	39.7	40.2	0.7
2007 Toyota Camry Hybrid	-1.4	35.2	35.2	4.7
2007 Chevy Tahoe	-17.8	46.3	49.6	-9.2
2007 Volkswagen Jetta	-4.4	34.6	34.9	1.7
2006 Honda Ridgeline	-16.2	43.7	46.6	-8.1
2006 Chrysler 300	-14.4	35.2	38.0	-7.8
2005 Volvo XC90	-10.1	42.1	43.3	-2.5

Given a situation in which the roof crush on the A-pillar of a vehicle is 6 inches and the roof crush on the B-pillar is 4 inches, the CG relative to the horizontal position of the virtual (undeformed) A-pillar was calculated and tabulated in column 5 of Table 3. Ten degrees of pitch was assumed given the 6 inches and 4 inches of roof crush on the A-pillar and B-pillar. In analyzing the data in column 5 from Table 3, the CG moves horizontally closer relative to the virtual A-pillar and in some cases moves forward of the pivot point causing the vehicle to want to pitch even further forward. Using the data for the horizontal distance between the CG relative to the A-Pillar at 10º of pitch and the residual crush for each respective vehicle in Roll 2 of the JRS test, a scatter plot was created and shown below in Figure 24.

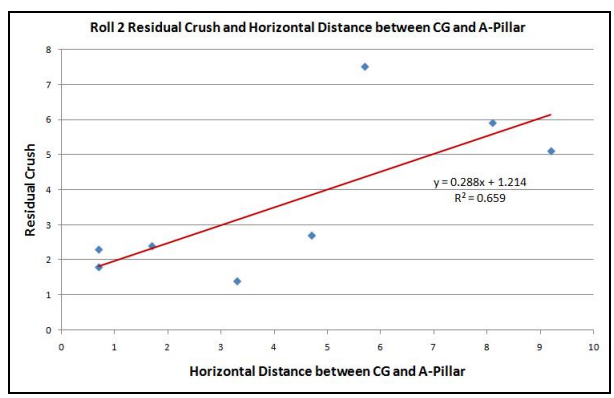

Figure 24. Roll 2 residual crush and horizontal distance between CG and A-pillar.

The data in Figure 24 implies that the greater the distance between the CG and the A-pillar at 10º of pitch, the more residual roof crush the vehicle experienced. The R^2 value of the linear regression

line is 0.659 meaning there is some correlation between the two. A further analysis shows Figure 24 only takes into consideration the magnitude of the distance between the CG and the A-pillar at 10º of pitch. The three vehicles that experience the most residual crush, the 2008 Scion xB, 2007 Chevy Tahoe, and the 2006 Honda Ridgeline, actually have their CG's behind the A-pillar at 10º of pitch. Their initial unloaded CG's are horizontally the farthest back of all the vehicle and even at 10º of pitch it is not enough to move their CG's forward of the A-pillar and pivot point. In reality these three vehicles are unlikely to roll with pitch because even at a forced pitch of 10º by the JRS, the CG, although it moves forward by a fair amount, is still behind the pivot point. From prior analyses we know that the 2008 Scion xB experiences a large residual crush due to its square profile and the 2007 Chevy Tahoe experiences large residual crush due to its weak roof structure with a SWR of 2.1 and because it has one of the largest major radiuses as shown previously in Figure 16 [20].

CONCLUSIONS

C*f*IR previously showed that residual crush decreases with SWR, ejection potential decreases with SWR greater than 3.0 and crush increases with 10° pitch. This analysis indicates that:

- Momentum derived hybrid III dummy injury measures (IBM) correlate with residual crush, injury risk and IARV injury measure criteria.
- Increased major radius results in increased injury potential independent of SWR,
- Elastic structures reduce injury potential.
- Increasing road speed and proportional roll rate increases injury potential
- Shifting CG Rearward (Rear seat passengers or load) reduces injury potential by reducing pitch propensity.

C*f*IR has proposed a real world rollover test protocol and demonstrated how to adjust (normalize) the 50 dynamic test already conducted to predict dynamic performance within any protocol. The University of Virginia sponsored by NHTSA has been given responsibility to developed a real world protocol. [21] By virtue of the relationships developed here, vehicle performance may be roughly predicted for most variations in the protocol.

Lessons Learned

Frontal impact protection The reduction in musculature and orientation of the Hybrid III neck as developed for rollover testing appears to explain anomalies in frontal and side impact protection. For instance the IIHS reported an increase in fatalities with advanced airbags compared to the immediately previous designs [22]. An identical set-up for frontal impacts at typical airbag deployment ignition speeds of 15 mph is shown with the Hybrid III dummy with its original and reduced musculature neck in Figures 25 and 26, respectively. The flexibility of the reduced musculature puts the dummy's head in close proximity to the deploying airbag with serious injury consequences if the airbag fires and from striking the wheel hub if it doesn't.

Figure 25. Hybrid III dummy with original musculature neck.

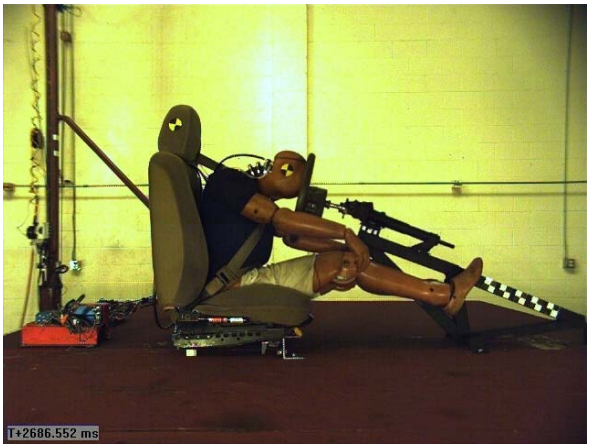

Figure 26. Hybrid III dummy with reduced musculature neck.

Side impact protection Window curtain airbags are now in use as head impact protection for side impacts and as such deploy at 100 to 120 mph. Rollover activated window curtain airbags for

ejection protection deploy at 25 to 50mph. If the side impact airbag is activated during a rollover because of the vehicle side being in proximity to the ground while the occupant is "up and out" against the roof rail the result may be head and brain trauma, diffuse axonal injury, and coma. A solution would be to have two or variable inflators and change the rollover sensing algorithm to override and inhibit the side impact deployment gas generator.

REFERENCES

[1] Brumbelow, M. and B. Teoh. 2009. "Roof Strength and Injury Risk in Rollover Crashes of Passenger Cars and SUVs." SAE Government Industry Meeting. February 2009.

[2] Tahan, F., K. Digges and P. Mohan. 2010. "Sensitivity Study of Vehicle Rollovers to Various Initial Conditions – Finite Element Model Based Analysis." ICRASH Conference, Washington, D.C., September 2010.

[3] J. Kerrigan, Government Industry Meeting PPT. 2009.

[4] http://www-nass.nhtsa.dot.gov/nass/cds-new/SearchForm.aspx

[5] http://nhtsa-nrdapps.nhtsa.dot.gov/bin/cirenfilter.dll

[6] Australian Transport Safety Bureau. "International Road Safety Comparisons: The 2004 Report – A Comparison of Road Safety Statistics in OECD Nations and Australia." 2006.

[7] Nash, C. and A. Paskin. 2005. "Rollover Cases with Roof Crush in NASS."2005 Summer Bioengineering Conference. Vail, Colorado. June 22-26, 2005.

[8] Bish, J., J. Caplinger, D. Friedman, A. Jordan, C. Nash. 2008. "Repeatability of a Dynamic Rollover Test System" ICRASH Conference, Kyoto, Japan, July 21-25, 2008.

[9] http://www.gm.com/company/corp_info/history/gmhis1970.html

[10] Ridella, S.A. and A.M. Eigen. 2008. "Biomechanical Investigation of Injury Mechanism in Rollover Crashes from the CIREN Database." IRCOBI Conference, Bern, Switzerland, September 17-19, 2008.

[11] Pintar, F.A., L.M Voo, et. al. 1998. "Mechanisms of Hyperflexion Cervical Spine Injury." IRCOBI Conference, Goteborg, September 1998.

[12] Paver, J.G. and D. Friedman, et. al. 2010. "The Development of IARV's for the Hybrid III Neck Modified for Dynamic Rollover Crash Testing." ICRASH Conference, Washington, D.C., September 22-24, 2010.

[13] Mertz, H.J, P. Prasad, et. al. 2003. "Biomechanical and Scaling Bases for Frontal and Side Impact Injury Assessment Reference Values." Stapp Car Crash Journal, Vol. 47, 155-188.

[14] Paver, J.G., et. al. 2008. "Rollover Roof Crush and Speed as Measures of Injury Potential vs. the Hybrid III Dummy." ICRASH Conference, Kyoto, Japan, July 22-25, 2008.

[15] Paver, J.G., et. al. 2008. "Rollover Crash Neck Injury Replication and Injury Potential Assessment," IRCOBI Conference, Bern, Switzerland, September 17-19, 2008.

[16] Moffatt, E.A. et. al. 2003. "Matched-Pair Rollover Impacts of Rollcaged and Production Roof Cars Using the Controlled Rollover Impact System (CRIS)." SAE World Congress Conference, 2003.

[17] Fildes, B. and K. Digges. 2009. "Occupant Protection in Far-Side Crashes" National Crash Analysis Center, GWU, Monash University Accident Research Centre, June 2009.

[18] Friedman, D., S. Bozzini, J. Paver. 2010. "Status of Comparative Dynamic Rollover Compliance Research and Testing." ICRASH Conference, Washington, D.C., September 22-24, 2010.

[19] Brumbelow, M. et. al., 2008. "Roof Strength and Injury Risk in Rollover Crashes." Insurance Institute for Highway Safety. March 2008.

[20] Friedman, D., G. Mattos, J.G. Paver. 2010. "Characterizing the Injury Potential of a Real World Rollover." ICRASH Conference, Washington, D.C., September 22-24, 2010.

[21] Kerrigan, J.R. et. al. 2008. "Test System, Vehicle, and Occupant Response Repeatability Evaluation in Rollover Crash Tests: The Deceleration Rollover Sled Test." ICRASH Conference, Washington, D.C., September 22-24, 2010.

[22] Brumbelow, M.L., E.R. Teoh, D.S. Zuby, A.T. McCartt. 2008. "Roof Strength and Injury Risk in Rollover Crashes." Insurance Institute for Highway Safety, March 2008.

[23] Rico, D. "Parameter Analysis" JRS Dynamic Correlations for IARV = 0.456 and for IBM =0.708

APPENDIX 1.

Vehicle	Headroom Measurement (inches)	Max. Lap Belt Load Roll 1 (lbs)	Max. Shoulder Belt Load Roll 1 (lbs)	Max. Lap Belt Load Roll 2 (lbs)	Max. Shoulder Belt Load Roll 2 (lbs)	Impact Angle, Roll Rate Roll 1	Impact Angle, Roll Rate Roll 2	Far Side Road Load Roll 1 (lbs)	Far Side Road Load Roll 2 (lbs)
2005 Volvo XC90	6.25	215	101	119	124	143º, 179º/sec	139º, 180º/sec	18,229	22.145
2007 VW Jetta	4.25	164	105	106	115	142º, 156/sec	143º, 172º/sec	17,362	20,798
2007 Toyota Camry	5	115	100	224	94	141º, 138º/sec	140º, 170º/sec	19,242	25,038
2007 Honda CR-V	4.25	123	102	126	119	143º, 196º/sec	141º, 209º/sec	16,115	14,264
2009 Nissan Versa	5	237	175	225	222	144º, 187º/sec	145º, 194º/sec	19,451	19,151
2006 Hyundai Sonata	4.5	127	93	200	190	143º, 133º/sec	145º, 166º/sec	17,711	31,380
2007 Toyota Camry (Hybrid)	5	177	136	154	123	143º, 180º/sec	136º, 185º/sec	20,024	28,919
2008 Scion xB	6.5	432	207	206	94	141º, 201º/sec	146º, 196º/sec	27,861	20,422
1998 Ford Explorer	3.75	104	69	62	7	146º, 183º/sec	143º, 186º/sec	15,964	25,624
2006 Pontiac G6	2.5	171	128	324	147	139º 172º/sec	140º, 175º/sec	19,062	33,406
2006 Honda Ridgeline	4.75	123	79	166	81	145º, 208º/sec	145º, 203º/sec	20,385	33,023
2006 Chrysler 300	4.5	137	101	539	127	146º, 161º/sec	147º, 156º/sec	24,001	43,085
2007 Chevrolet Tahoe	5.25	192	140	244	64	142º, 213º/sec	143º, 210º/sec	24,727	39,575
2007 Pontiac G6	4.75	87	92	N/A	N/A	142º, 172º/sec	N/A	19,185	N/A
2007 Jeep Grand Cherokee	3.5	125	91	30	10	147º, 197º/sec	149º, 190º/sec	23,908	32,293
2004 Volvo XC90 (White)	N/A	N/A	N/A	N/A	N/A	133º, 214º/sec	148º, 215º/sec	13,590	15,461
2004 Subaru Forester (Red)	N/A	N/A	N/A	N/A	N/A	147º, 223º/sec	150º, 139º/sec	14,723	15,756
2004 Land Rover Discovery II	N/A	122	102	74	38	136º, 212º/sec	145º, 207º/sec	13,608	10,240
2003 Subaru Forester (Tan)	N/A	N/A	N/A	125	114	147º, 212º/sec	151º, 173º/sec	15,283	13,151
2003 Subaru Forester (Green)	N/A	N/A	N/A	113	122	N/A	143º, 174º/sec	14,764	13,912
2002 Toyota Corolla	N/A	N/A	N/A	N/A	N/A	132º, 178º/sec	145º, 176º/sec	8,448	8,626
2001 Chevrolet Suburban	N/A	197	31	N/A	N/A	140º, 214º/sec	N/A	18,579	N/A
2000 GMC Jimmy	5	73	67	N/A	N/A	146º, 174º/sec	N/A	17,455	N/A
2000 Ford Explorer	N/A	N/A	N/A	N/A	N/A	134º, 200º/sec	144º, 188º/sec	9,263	14,251
1999 Oldsmobile Bravada	4.5	N/A	N/A	139	59	149º, 19º/sec	147º, 184º/sec	19,613	29,274
1999 Jeep Grand Cherokee	3	63	31	N/A	N/A	147º, 257º/sec	N/A	24,268	N/A
1999 Isuzu Vehicross	N/A	N/A	N/A	N/A	N/A	139º, 185º/sec	148º, 183º/sec	9,409	15,701
1999 Hyundai Sonata (Black-20.8mph)	4.5	68	29	N/A	N/A	145º, 275º/sec	N/A	20,232	N/A
1999 Hyundai Sonata	N/A	N/A	N/A	N/A	N/A	139º, 172º/sec	148º, 157º/sec	9,466	10,779
1998 MB ML320	4	N/A	97	N/A	N/A	144º, 231º/sec	N/A	17,143	N/A
1997 Chevrolet Cavalier	2.75	95	149	N/A	N/A	142º, 231º/sec	N/A	20,577	N/A
1997 Acura CL 2.2	4	136.6	76.3	N/A	N/A	144º, 205º/sec	N/A	15,351	N/A
1996 Isuzu Rodeo	8.75	74.3	78.7	N/A	N/A	148º, 239º/sec	N/A	18,946	N/A
1993 Jeep Grand Cherokee	4.75	160	N/A	N/A	N/A	148º, 244º/sec	N/A	25,068	N/A